Defence Science Journal, Vol. 59, No. 1, January 2009, pp. 22-29

REVIEW PAPER

Dynamic Behaviour of Concrete Sandwich Panel under Blast Loading

Dong Yongxiang[1], Feng Shunshan[1], Xia Changjing[2], and Gui Lele[2]

[1]*Beijing Institute of Technology, Beijing China-100 081*
[2]*China University of Mining & Technology, Beijing, China-100 083*

ABSTRACT

Surface contact explosion experiments were performed to study the dynamic behaviour of concrete sandwich panel subjected to blast loading. Experimental results have shown that there are four damage modes explosion cratering, scabbing of the backside, radial cracking induced failure, and circumferential cracking induced failure. It also illustrates that different foam materials sandwiched in the multi-layered medium have an important effect on damage patterns. Due to the foam material, the stress peak decreases one order of magnitude and the duration is more than four times that of the panel without the soft layer by numerical simulation. Additionally, the multi layered medium with concrete foam demonstrates the favourable protective property compared with that of aluminum foam. Meanwhile, the optimal analysis of the thickness of the foam material in the sandwich panel was performed in terms of experimental and numerical analyseis. The proper thickness proportion of soft layer is about 20 percent to the total thickness of sandwich panel under the conditions in this study.

Keywords: Dynamic behaviour, concrete sandwich panel, blast loading, foam material

1. INTRODUCTION

Eytan[1] proposed the design of layered structures against the conventional weapons. Tedesco[2], *et al*. pointed out that a layered structure can effectively protect targets against attack and the proper combination of different materials can weaken the explosion wave. Moreover, protective abilities of three Layered structures of concrete-air-concrete, concrete-polystyrene-concrete and concrete-soil-concrete were compared applying numerical simulation. The results show that each structure can reduce or eliminate the scabbing of the inner wall of the structure. Tedesco[3], *et al*. further investigated the protective role of the laminated structure against the conventional weapons. Study on wave reflection and transmission of the layered interface, indicated that mismatching of material wave impedance had significant effect on the attenuation of stress wave. Franz[4], *et al*. conducted the study on the dynamic behaviour of glass fibre laminated medium under blast loading by experiments. The result showd that the media with low impedance and high energy absorption can be used as the protective materials to withhold explosion loading near the explosive charge. The material with high strength and high bending resistance can be used around the protected objects. These conclusions provide guidance for the design of multi-layered protective structures. The penetration of projectile into composite targets was carried out using numerical method by Gupta[5], *et al*. The results show that the *SiC* medium with high wave impedance and high wave speed can lead the applied load to spread transversely and effectively transmit much more energy to the next layer.

From the above state, it is implied that the multilayered structure with the lower wave impedance material as the middle layer can reduce the intensity of impact and blast loading effectively. The dynamic response of sandwich panel including low wave impedance foam materials and the different thickness and position of foam materials under explosive loading has been studied.

2. ANALSYSIS ON SANDWICH PANEL WITH DIFFERENT FOAM MATERIALS

2.1. Explosion Experiment

The experimental setup is shown in Fig. 1. The cylindrical emulsion explosive with a mass m_e of 300g was put on the top surface of three-layered media. To effectively reduce the damage of sandwich panel[6,7], Layer-I and Layer-III were the reinforced concrete. Layer-II was the foam material. The three layers were only stacked up. The sandwich panel with concrete foam (C-CF-C) and the sandwich panel with aluminum foam

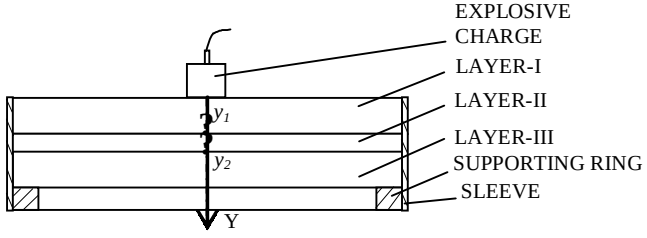

Figure 1. Sketch of experimental setup.

Received 20 December 2007, revised 01 July 2008

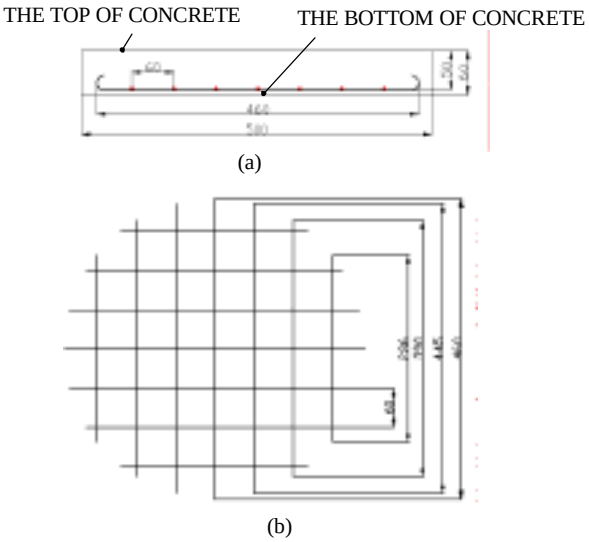

(a)

(b)

Figure 2. Reinforcement details for concrete panel (Unit: mm): (a) Cross-section view of reinforced concrete; (b) Top view of steel bars.

(C-*AlF*-C) are employed for study of dynamic behaviour of the sandwich panel with different middle layers. The thickness of the three wave layer is 6 cm, 3 cm, and 6 cm, respectively. The diameter of sandwich panel was 50 cm which is more than triple the thickness of sandwich panel. Figure 2 shows the reinforcement details for concrete panel. The steel bars form the square grids that are 60 mm x 60 mm.

The ratio of reinforcement was 0.77 per cent and the diameter of the steel bars for the reinforced concrete was 6.5 mm. The coordinate system was established as shown in Fig. 1.

2.2 Failure Phenomena of Sandwich Panel

The damage profiles of sandwich panel C-CF-C and C-*AlF*-C after explosion are shown in Figs 3 and 4. In Fig. 3(a), one can clearly observe a crater, formed in the centre of the upper layer, a spalling region on the front surface, and much radial cracking and circumferential cracking adjacent to the spalling. The diameter of spalling was about 28 cm (the average diameter is adopted as the diameter of spalling, undermentioned diameters of different zones are obtained similarly), just as shown in Table 1. Figure 3(b) shows that many radial cracks are formed on the backside of the lower layer and the scabbing occurs at the lower surface because the reflected wave reaches tensile strength of concrete. Correspondingly, Fig. 4(a) shows a rather large size of crush fragments and a small amount of cracks compared to that of the front side upper layer for C-CF-C specimen. The diameter of scabbing shown in Fig. 4(b) is smaller than 15 cm. Figures 5 and 6 present damage profiles of the

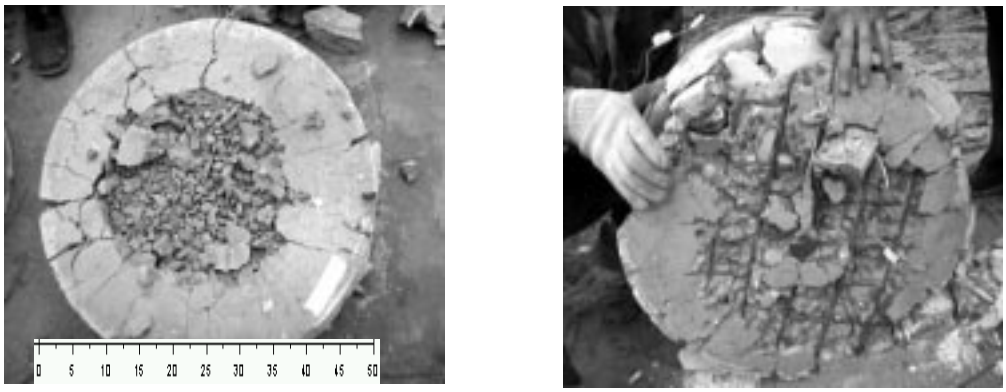

(a) (b)

Figure 3. Photographs of C-CF-C specimen after explosion: (a) The front of upper concrete; (b) The back of lower concrete.

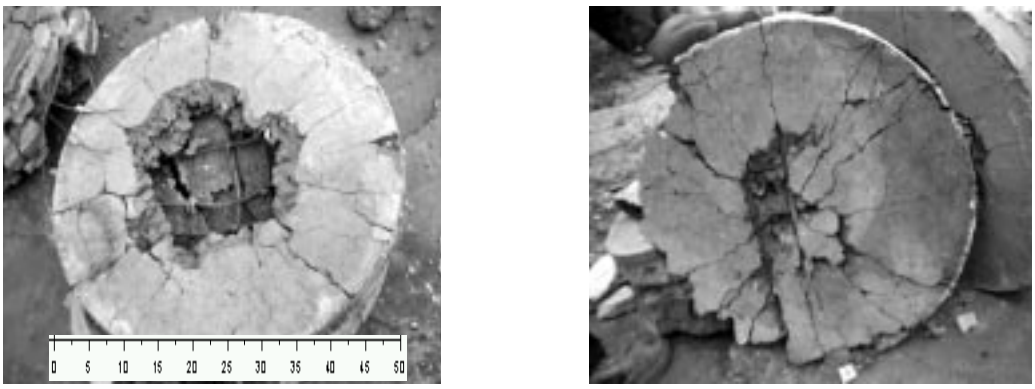

(a) (b)

Figure 4. Photographs of C-AlF-C specimen after explosion: (a) The front of upper concrete; (b) The back of lower concrete.

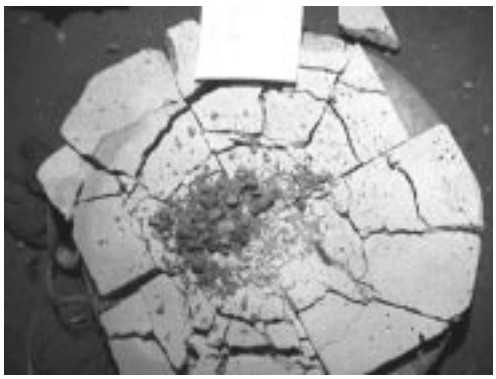

Figure 5. Damage profile of concrete foam.

Figure 6. Damage profile of aluminum foam.

Table 1. Experimental results of different foam layer

Specimens	Foam materials	m_e (g)	Failure and damage	
			The front of upper concrete	The back of lower concrete
C-CF-C	Concrete foam	300	Spalling dia ~ 28 cm crater dia ~ about 27 cm	Scabbing dia ~ 32 cm
C-*AlF*-C	Aluminum foam	300	Spalling dia ~ 25 cm crater dia ~ 19 cm	There are many circumferential cracks. Scabbing dia < 15 cm

middle concrete foam and aluminum foam layers after explosion. Many radial and circumferential cracks on the top surface indicate that the stress peak value greatly exceeds compressive strength of concrete foam in Fig. 5. In summary, two kinds of specimens have different damage and failure modes and the C-*AlF*-C sandwich tends to localised failure compared with C-CF-C specimen.

2.3 Numerical Simulation

Here, some numerical results are presented to illustrate characteristics of wave propagation and dynamic behaviour of sandwich panel under blast loading. The calculation was carried out in 2D axisymmetric configuration with an available computer program LS-DYNA. The Lagrange algorithm was adopted in the calculation to compare energy loss with that of ALE (Arbitrary Lagrangian-Eulerian) algorithm. When blast pressure was approximately zero, explosive would be deleted and the computation was performed continuously. The JWL equation of state was adopted to describe the behaviour of the explosion product. In the calculation, the reinforced concrete was simplified as plain concrete according to the equivalent strength. Johnson-Holmquist (JH) constitutive model was used for concrete[8,9], crushable-foam model[10] was applied for foam materials. Material parameters are listed in Tables 2 to 4. Here ρ and E are density and elastic modulus, D_H, the detonation velocity, P_{CJ}, the C-J detonation pressure, E_0, the internal energy per unit volume, μ , Poisson ratio, and A, B, R_1, R_2, ω are material constants of JWL equation. In Table 3, G is the shear modulus and σ_c is the uniaxial compressive strength. In Table 4, T_{SC} is the cut off of tensile stress and D_{amp} the damping coefficient of the material. The stress-strain relation for concrete foam and aluminum foam are shown in Fig. 7. The dynamic response of foam materials from the works reported from refrences 11 to 16 was helpful in carrying out the simulation in this study.

Figure 8 shows pressure contours of C-*AlF*-C specimen at different times. When the explosive is ignited, explosion wave in the shape of approximate semicircle begins to propagate in the layer I. At 40 μs, explosion wave has reached the middle layer, and pressure fringes do not keep the semicircles due to the various wave speeds of the different material wave impedances. Explosion pressure wave moves down the different layers, and then is reflected and transmitted

Table 2. Material parameters of the emulsive explosive

ρ (g/cm^3)	D_H (m/s)	P_{CJ} (GPa)	A (GPa)	B (GPa)	R_1	R_2	ω	E_0 (GPa)
1.31	5500	9.9	214.4	0.182	4.2	0.9	0.15	4.19

Table 3. Main Equivalent material parameters of reinforced concrete

ρ(g/cm^3)	E (GPa)	μ	G (GPa)	σ_c (MPa)	Tensile strength, σ_t (MPa)
2.46	22.60	0.2	18.0	30	4.0

Table 4. Material parameters of foam materials

Material properties	Concrete foam	Aluminum foam
ρ(g/cm^3)	0.72	0.80
E (MPa)	2.70e+02	5.0e+02
μ	0.18	0.21
T_{SC} (MPa)	6.0	11.0
Damp	0.2	0.2

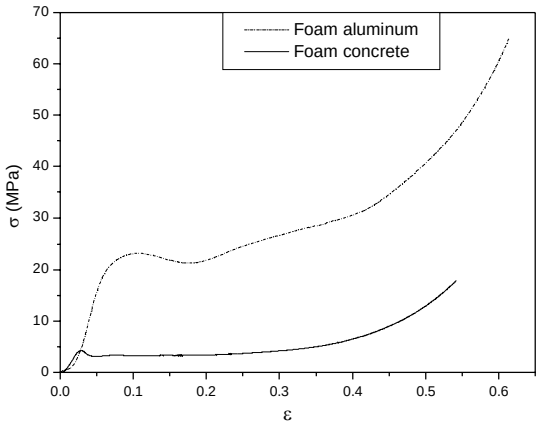

Figure 7. Stress-strain curves for foam materials.

at each boundary interface, interact and superpose when these encounter. For different materials, the decreasing sequence of wave impedance is $(\rho C)_C$, $(\rho C)_{A1F}$ and $(\rho C)_{CF}$, the subscripts C, *AlF* and CF denote reinforced concrete, aluminum foam, and concrete foam, respectively. At 75 μs, it illustrates that

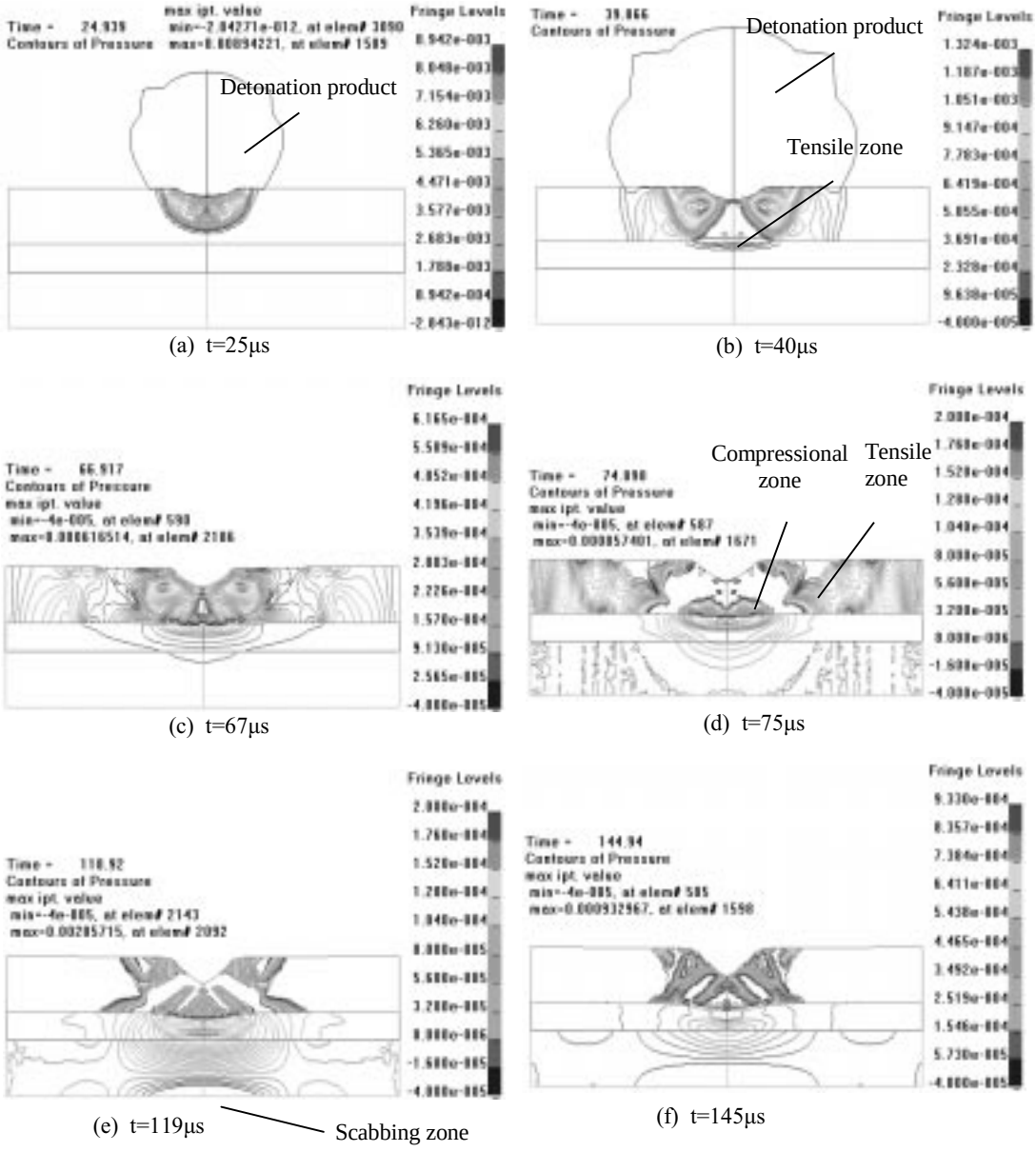

(a) t=25μs (b) t=40μs

(c) t=67μs (d) t=75μs

(e) t=119μs (f) t=145μs

Figure 8. Calculated pressure profiles with time sequence in C-AlF-C model (Unit: 10^5MPa).

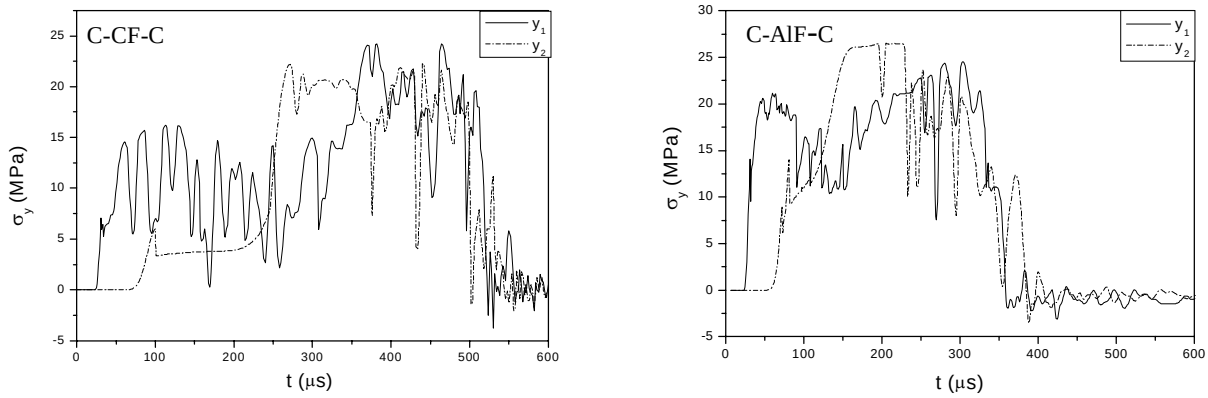

Figure 9. Stress σ_y versus time *t* in *C-CF-C* and *C-AlF-C* models.

the closer to the charge, the larger is the compression zone. From the computed result at 119 μs, compression wave reaches the bottom of lower layer, tensile wave is reflected from the free rear surface and the scabbing zone occurs.

The damage and failure profiles of sandwich panel are also obtained from pressure contours in Fig. 8. The tensile and spalling zones are formed when explosion wave propagates and interacts in different layers at different times, just marked as in Figs 8(b) to (e). From numerical results it can be obtained that crater diameter in the front of upper layer is 16 cm, spalling diameter is 26 cm, and scabbing diameter on the backside of low concrete is 18 cm for C-*AlF*-C specimen. Those are approximately in agreement with experimental results. For C-CF-C specimen, the crater diameter in the front of upper layer is 20 cm, spalling diameter is 28 cm, and the scabbing diameter on the back of low concrete is about 36 cm.

Figure 9 shows the curves of stress σ_y versus time at different points y1 and y2, which are located on the axial line and contact interfaces with middle layer, as shown in Fig. 1. Figure 10 shows the typical stress σ_y versus time at corresponding positions of 3C model in which the middle layer is replaced by the same reinforced concrete. There obviously exists different stress wave in different sandwich panels. The pressure peak value is slightly lower and the duration is longer in *C-CF-C* specimen compared to that of *C-AlF-C* specimen. Obviously, the peak stress σ_y of sandwich panel decreases about one order of magnitude than that of 3C model (shown in Fig. 10), and the duration is more than four times as percentage as that of 3C model. Thus the multilayered media with foam material layer can not only reduce the stress peak value effectively, but can also change the duration of the explosion wave.

Curves of absorbing energy per unit area E_{ab} of layer II and layer III with time are shown in Fig. 11 to compare the influence of different foam materials. The absorbing energy of layer II of *C-AlF-C* specimen is lower than that of *C-CF-C* specimen. On the contrary, absorbing energy of layer III of *C-AlF-C* specimen is higher than that of *C-CF-C* specimen. Because of its longer duration, *C-CF-C* sandwich specimen is more favorable than *C-AlF-C* specimen in the protective design associated with the experimental results.

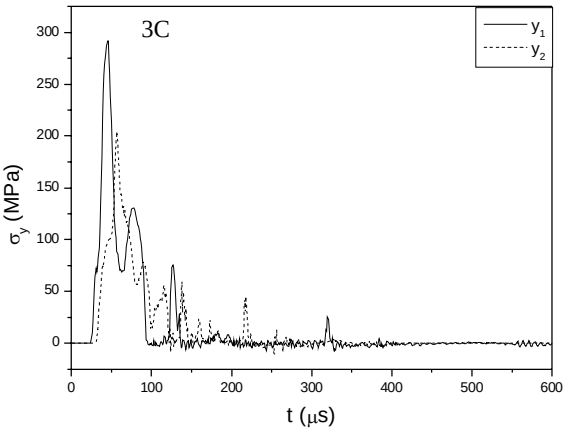

Figure 10. Stress σ_y versus time *t* in 3C model.

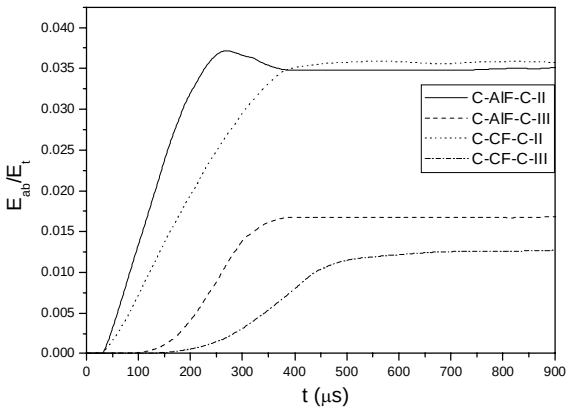

Figure 11. Curves of absorbing energy E_{ab} of layer-II and layer-III versus time *t* in different model.

3. OPTIMAL ANALYSIS OF FOAM LAYER THICKNESS

Foam materials with different thickness in the multilayered media have different antidetonation performances. On the condition of the same amount of the explosive charge, the same total thickness of sandwich panel and the thickness of the upper layer equal to that of the lower layer, the influence of foam material thickness on damage of sandwich panel was analysed by *C-CF-C* specimens. The experimental results are summarised in Table 5. Here h_1, h_2, and h_3 are the

Table 5. Experimental results of different foam layer thickness

C-CF-C Specimens	h_1 (cm)	h_2 (cm)	h_3 (cm)	m_e (g)	Failure and damage	
					Front of upper concrete	Back of lower concrete
(A)	7.0	1.0	7.0	250	Crater dia ~ 23 cm	Scabbing dia ~ 32 cm
(B)	6.5	2.0	6.5	250	Crater dia ~ 25 cm	Scabbing dia ~ 29 cm
(C)	5.5	4.0	5.5	250	Crater dia ~ 20 cm	Scabbing dia ~ 8 cm
(D)	6.0	3.0	6.0	280	Spalling dia ~ 22 cm	There exist radial cracks, but no scabbing zone

(a) (b)

Figure 12. Photographs of *C-CF-C*(*C*) specimen after explosion: (a) the front of upper concrete; (b) the front of lower concrete.

(a) (b)

Figure 13. Photographs of *C-CF-C*(*D*) specimen after explosion: (a) the front of upper concrete; (b) the front of lower concrete.

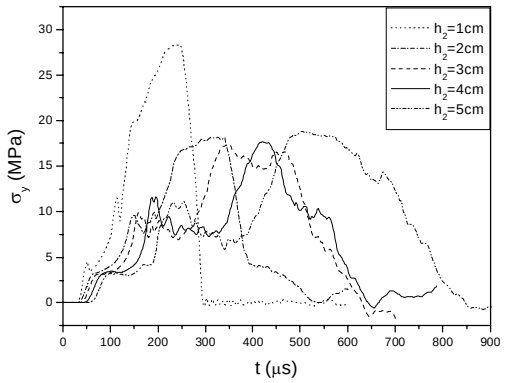

Figure 14. Stress σ_y curves of different concrete foam thickness versus time.

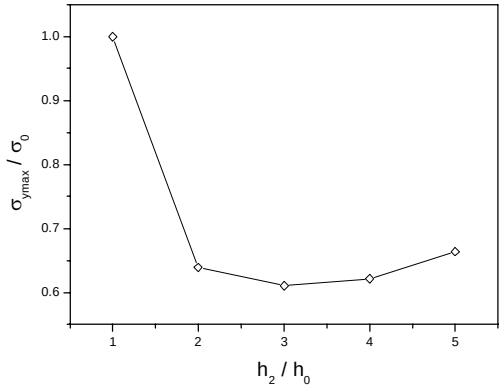

Figure 15. Curve dimensionless of σ_{ymax} with the thickness of concrete foam.

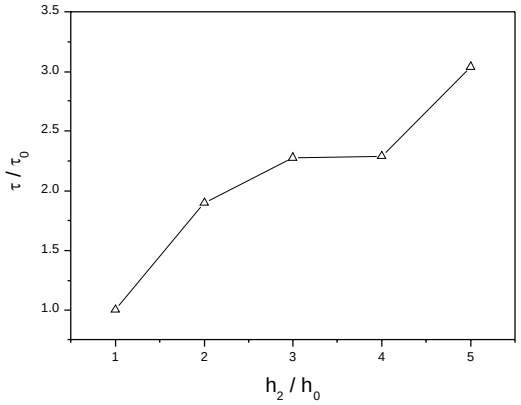

Figure 16. Curve of τ with the thickness of concrete foam.

thicknesses of the upper layer, middle concrete foam layer, and lower layer, respectively.

Typical photographs of experimental results are shown in Figs 12 and 13. These photographs illustrate reinforced concrete damage and failure profiles of *C-CF-C*(*C*) and *C-CF-C*(*D*) specimens after explosion. Compared with Fig. 3, *C-CF-C*(*D*) specimen can be subjected to more explosive charge, but slighter damage than that of other groups only occurs. It is found that when the ratio of foam thickness to the total thickness is 1:5, the anti-detonation ability of the sandwich panel is the optimal.

On the condition of the same amount of the explosive charge m_e equal to 250 g, numerical simulation was carried out. The material models and parameters were the same as in the previous computation.

Figure 14 shows stress curves of different concrete foam thicknesses versus time at the middle point of foam layer. Figures 15 and 16 show curves of dimensionless maximum stress and duration versus the thickness of foam layer. To obtain dimensionless parameters, here the fundamental magnitude σ_0, t_0 and h_0 are chosen as the corresponding values when concrete foam thickness h_2 equals to 1 cm. The tendency of stress curves verified that when the ratio of foam layer thickness to the thickness of sandwich panel was 1:5, which is in agreement with the experimental results.

4. CONCLUSIONS

This paper presents the analysis on dynamic behaviour of a sandwich panel under explosive loading. From the experimental and computational results, the low wave impedance foam material of the middle layer plays an important role on bearing explosion loading. The peak stress decreases, the duration becomes longer, and energy distribution of different layers change due to the foam layer. Concrete foam sandwiched in a layered media has more influence on protective performance to blast loading than that of aluminum foam. It was also deduced that there exists the optimal thickness of the foam layer relative to the whole sandwich panel. In practice, there exists a strong coupling effect between blast loading and layered structures. So, it is necessary to carry out further study on the coupling of the charge and concrete sandwich panel in the near future.

ACKNOWLEDGEMENTS

The authors would like to thank Prof Z.P. Duan, of Institute of Mechanics, Chinese Academy of Sciences, for the helpful discussions. This work was performed with the help of China University of Mining and Technology Beijing. This work was sponsored by Open Foundation of State Key Laboratory of Explosion Science and Technology of Beijing Institute of Technology.

REFERENCES

1. Eytan, R. Design of layered structures against conventional weapons. *In* Proceedings of the Second International Symposium on Interaction of Non-Nuclear Munitions with Structures. Panama City Beach, Florida, USA, 1985.
2. Tedsco, J.W.; Hayes, J.R.; et al. Dynamic response of layered structures subject to blast effects of non-nuclear weaponry. *Comput. Struct.,* 1987; **26**: 79-86.
3. Tedsco, J.W. & Landis, D.W. Wave propagation through layered systems. *Comput. Struct.* 1989; **26**: 625-38.
4. Franz, T.; Nurick, G.N.; et al. Experimental investigation into the response of chopped strand mat glassfibre laminates to blast loading. *Int. J. Impact. Eng.*, 2002; **27**: 639-67.
5. Gupta, Y.M. & Ding, J.L. Impact load spreading in layered materials and structures: concept and quantitative measure. *Int. J. Impact. Eng.*, 2002; **27**: 277-91.
6. Wu CQ, Hao H. Numerical simulation of structural response and damage to simultaneous ground shock and airblast loads. Int J Impact Eng 2007; 34:556-572.
7. Joosef, L. Dynamic behaviour of concrete structures subjected to blast and fragment impacts. PhD dissertation, Chalmers University of Technology, Sweden, 2002.
8. Timothy, J.H.; Douglas, W.T.; et al. Constitutive modeling of aluminum nitride for large strain, high-strain rate, and high-pressure applications. *Int. J. Impact. Eng.*, 2001; **25**: 211-31.
9. Song, S.C.; et al. SPH algorithm for projectile penetrating into concrete. Explosion and shock waves (in Chinese) 2003; **23**(1): 56-60.
10. Hallquist, J. LS-DYNA Keyword user's manual. Livermore Software Technology Corporation, 2001.
11. Taylor, E.A.; Tsembelis, K.; et al. Hydrocode modeling of hypervelocity impact on brittle materials: depth of penetration and conchoidal diameter. *Int. J. Impact. Eng.* 1999; 23: 895-904.
12. Grote, D.L.; Park, S.W.; et al. Dynamic behavior of concrete at high strain rates and pressures: I. Experiment characterization. *Int. J. Impact. Eng.*, 2001; **25**: 869-86.
13. Xu, Z.X. Influence of the duration of the severe ground movement on the collapse of the structure. Journal of Tongji University (in Chinese) 1982; **2**: 7-23.
14. Cliffton, R.J. Stress wave propagation, dynamic material response, and quantitative non-destructive evaluation. *Appl. Mech. Rev.,* 1985; **38**: 1276-278.
15. Carruthers, J.J.; Kettle, A.P.; et al. Energy absorption capability and crashworthiness of composite material

structures: A review. *Appl. Mech. Rev.*, 1989; **51**(10): 635-49.

16. Santosa, S.P.; Wierzbicki, T.; et al. Experimental and numerical studies of foam-filled sections. *Int. J. Impact Eng.*, 2000; **24**: 509-34.

Contributors

Dr Dong Yongxiang obtained her PhD from Institute of Mechanics, Chinese Academy of Sciences in 2004. She joined the State Key Laboratory of Explosion Science and Technology, Beijing Institute of Technology as a teacher in the same year. Her research interests are in explosion dynamics, impact dynamics and explosion protection.

Mr Feng Shunshan obtained his master's degree from the Beijing Institute of Technology in 1982. Now, he is a professor and the leader in his chosen field of learning at State Key Laboratory of Explosion Science and Technology. His research interest includes the explosive effect and its protection.

Mr Xia Changjing obtained his PhD from the University of Science and Technology of China in 2003. Now he joined the School of Mechanics & Civil Engineering, China University of Mining & Technology in 2005. At present, he is working as an Associate Professor and his research interest is in rock mechanics and explosion dynamics.

Mr Gui Lele graduated from the Hefei University of Technology in 2003. He is a graduate student for Masters from the School of Mechanics & Civil Engineering, China University of Mining & Technology. His research interest includes rock mechanics.